

# Weld Effective Lengths For Rectangular HSS Overlapped K-Connections

KYLE TOUSIGNANT and JEFFREY A. PACKER

---

## ABSTRACT

One large-scale, 33-ft-span, simply supported Warren truss was tested to assess the performance of welds in rectangular hollow structural section (HSS) overlapped K-connections. Nine overlapped connections, within the truss, were designed to be weld-critical and sequentially failed by producing an axial force distribution with a point load, applied quasi-statically, to strategic panel points. The structural reliability (or safety index) of the existing AISC *Specification* formulas for the effective length of welds in rectangular HSS overlapped K-connections, in Table K4.1 of the 2010 AISC *Specification for Structural Steel Buildings*, was determined from the tests. The results indicate that these provisions are conservative; hence, a modification to the current requirements that limits the effective width of the transverse weld elements is proposed. The proposal establishes a more economical and yet still safe weld design method for rectangular HSS overlapped K-connections.

**Keywords:** hollow structural sections, welded joints, trusses, K-connections, weld effective lengths, fillet welds, flare-bevel-groove welds, flux-cored arc welding.

---

## INTRODUCTION

It is well known that the differences in relative stiffness of rectangular hollow structural section (HSS) walls cause nonuniform load transfer along lines of welds at a branch connection. Historically, international design recommendations have required that these welds be designed to develop the yield strength of the member, such that they may resist any arrangement of loads in the branch. This requirement is almost exclusively based on old recommendations from the International Institute of Welding (IIW, 1989). Designing welds to branches to develop the yield strength of the member is justifiable in situations when there is low confidence in the design forces or if plastic stress redistribution is required in the connection (Packer et al., 2009). This design method is not always merited, and its requirement for large weld sizes is excessively conservative in many situations.

Extensive laboratory tests have been performed at the University of Toronto on welds in both isolated rectangular HSS connections and complete trusses (Frater and Packer, 1992a, 1992b; Packer and Cassidy, 1995; McFadden et al., 2013; McFadden and Packer, 2014), which have led to the development, and international recognition (IIW, 2012;

ISO, 2013), of a more modern design approach based on actual branch member forces to achieve more appropriate and economical weld sizes. This so-called fit-for-purpose approach makes use of effective weld properties to account for the nonuniform loading of the weld perimeter.

In the latest edition of AISC 360, *Specification for Structural Steel Buildings* (AISC, 2010), a detailed design method considering effective weld properties for predominantly statically loaded rectangular HSS-to-HSS connections is given in Section K4: “Welds of Plates and Branches to Rectangular HSS.” Table K4.1, “Effective Weld Properties for Connections to Rectangular HSS,” contains formulas to determine the effective length of welds for axially loaded rectangular HSS connections and the effective elastic section modulus of welds subject to bending.

The design methods in Table K4.1 for welds in axially loaded T-, Y-, X- and gapped K-connections are based on experimental data from full-scale tests on connections in which failure occurred by shear rupture of the weld along a plane through the weld throat, herein called “weld-critical connections” (Frater and Packer 1992a, 1992b; Packer and Cassidy, 1995). However, at the time that AISC 360-10 was published, no such data were available to substantiate the design methods given, in the same document, for welds in unreinforced HSS moment T-connections and axially loaded HSS overlapped K-connections.

In order to evaluate the adequacy of these design methods, AISC initiated a two-phase study at the University of Toronto. The first phase of the study investigated the strength and behavior of welds in unreinforced rectangular HSS moment T-connections. The results of this phase have been published by McFadden and Packer (2014). Phase two of the study is presented herein.

---

Kyle Tousignant, Ph.D. Candidate in Civil Engineering, University of Toronto, Toronto, Ontario, Canada. E-mail: kyle.tousignant@mail.utoronto.ca

Jeffrey A. Packer, Bahen/Tanenbaum Professor of Civil Engineering, University of Toronto, Toronto, Ontario, Canada (corresponding). E-mail: jeffrey.packer@utoronto.ca

---

Paper No. 2014-24

## EXPERIMENTATION

### Scope

An experimental program was developed to test large-scale rectangular HSS overlapped K-connections in order to verify, or adjust, the current weld effective length rules defined by Equations K4-10, K4-11 and K4-12 in Table K4.1 of the AISC *Specification* (AISC, 2010). Nine overlapped, 60-degree K-connections within one large-scale, 33-ft-span, simply supported Warren truss were designed to be weld-critical under the application of tension to the overlapping branch. Key parameters, such as the branch member overlap ( $O_v$ ), the branch-to-chord width ratio ( $\beta$ -ratio) and the chord wall slenderness ( $B/t$ ), were investigated and varied within the Limits of Applicability of Section K2.3 of the *Specification*. The nonuniform distribution of normal strain in the branch, near the connection, was measured with strain gages oriented along the longitudinal axis of the member at uniform increments around its perimeter, and the weld strength was obtained directly from strain gages in the constant stress region of the branch. To induce weld rupture, a single point load was applied to various truss panel points in a quasi-static manner. The loading strategy was carefully planned to accentuate the force in the critical web member(s) and resulted in all nine joints failing by shear rupture along a plane through the weld.

### Truss Design

#### General

Connections were welded using a semi-automatic flux-cored-arc-welding (FCAW) process with full  $\text{CO}_2$  shielding gas and fabricated from members conforming to CAN/CSA

G40.20/G40.21 Class C (CSA, 2013) and ASTM A1085 (ASTM, 2013). The experimental test designations, and a summary of the key test parameters for each joint ( $O_v$ ,  $\beta$  and  $B/t$ ), are given in Table 1.

The amount of overlap was varied, from 30% to 90%, and chord member sections were selected that produced relatively rigid and flexible connections. Connections were made to an HSS7 $\times$ 7 $\times$ 1/2 chord, that were relatively rigid ( $\beta = 0.71$  and  $B/t = 14.2$ ) and to an HSS10 $\times$ 10 $\times$ 3/8 chord that were more flexible ( $\beta = 0.50$  and  $B/t = 27.5$ ). Web members (HSS5 $\times$ 5 $\times$ 5/16) were specified to minimize the ratio of predicted weld strength to connection resistance and to also allow, by virtue of matched-width web members, either side of the truss connection to be designated as the overlapping (or “test”) branch. The latter detail was intended to support the design of a loading sequence to achieve sequential rupture of welds within the truss (see “Loading Strategy”).

Complete truss testing has been the preferred approach for testing welds in K-connections because it correctly accounts for connection boundary conditions, i.e., member continuity and truss deflection effects (Frater and Packer, 1992a, 1992b, 1992c). The truss layout and its dimensions are shown in Figure 1.

#### Weld Joint Details

The test welds were those to the overlapping branches, and each was comprised of three distinct weld joint details (see Figure 2): a longitudinal 90-degree fillet-weld detail (side a), a transverse 60-degree fillet-weld detail (sides c and d) and a longitudinal partial-joint-penetration (PJP) flare-bevel-groove-weld detail (side a’). The PJP flare-bevel-groove weld is formed by the butt joint in the matched-width web member connection. In this region, the deposition of sound

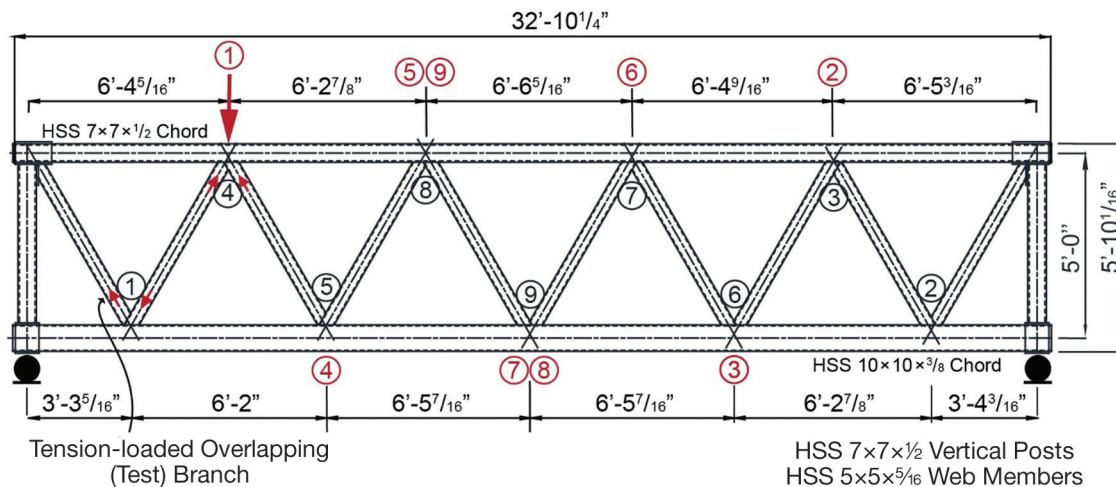


Fig. 1. Elevation of the truss, dimensions and joint designations (load locations for the nine tests shown in red; connection numbers shown in black).

Table 1. Measured Properties of Nine Rectangular HSS Overlapped K- (Test) Connections										
No.*	Test	HSS Web Member			HSS Chord Member			$O_v$ %	$\beta$	$B/t$
		$B_b \times H_b \times t_b$ in. $\times$ in. $\times$ in.	$A_b^{**}$ in. <sup>2</sup>	$F_{yb}^{***}$ ksi	$B \times H \times t$ in. $\times$ in. $\times$ in.	$A^*$ in. <sup>2</sup>	$F_y^{***}$ ksi			
1	K-90-0.50a	5.00 $\times$ 5.00 $\times$ 0.306	5.62	59.7	10.02 $\times$ 10.02 $\times$ 0.364	13.65	56.1	90	0.50	27.5
5	K-90-0.50b							90		
2	K-60-0.50							60		
6	K-30-0.50a							30		
9	K-30-0.50b							30		
3	K-90-0.71	5.00 $\times$ 5.00 $\times$ 0.306	5.62	59.7	7.03 $\times$ 7.03 $\times$ 0.494	12.05	55.1	90	0.71	14.2
4	K-60-0.71a							60		
7	K-60-0.71b							60		
8	K-30-0.71							30		
—	T2 Joint 4 <sup>†</sup>	5.03 $\times$ 5.03 $\times$	—	60.3	8.03 $\times$ 8.03 $\times$	—	52.1	50	0.63	17.4
—	T2 Joint 6 <sup>†</sup>	0.465	—	60.3	0.461	—	52.1	50	0.63	17.4

Note:  $\theta_i = \theta_j = 60^\circ$ ; and  $B_{bi}/t_{bi} = 16.3$  for connections 1–9.

\* Refer to Figure 1.

\*\* Cross-sectional areas determined by cutting a prescribed length of HSS, weighing it, and then using a density of 0.2836 lb/in<sup>3</sup> to calculate its cross-sectional area.

\*\*\* Yield strength of all HSS determined from tensile coupon tests performed according to ASTM A370 (2009).

† Tests by Frater (1991); failed by a combined mechanism of weld fracture and premature branch yielding.

weld metal to the bottom of the flare can be hindered by bridging the weld puddle between the surfaces of the two branches (Packer and Frater, 2005). Thus, the throat of such welds can be highly variable. It should be noted that correct input for the geometric and mechanical properties of the as-laid welds is requisite to the following analysis; thus, to establish a more reliable (precise) picture of the weld throat in this region, a complete penetration (CP) detail was specified (with a 1/4-in. root gap and backing) and subsequently qualified in accordance with Clause 4.13 of AWS D1.1 (2010). The weld details are shown in Figure 2.

All critical test welds (to the overlapping branches at the connections), with the exception of weld element c, were

performed in the horizontal position. Weld element c was performed in the flat position. Minimum weld sizes, as specified in Table 5.8 and Table 3.4 of AWS D1.1 (2010) and Table J2.4 and Table J2.3 of AISC 360 (2010) for fillet welds and PJP flare-bevel-groove welds, respectively, were used to ensure enough heat input during welding to establish a sound weld. The hidden toe of the overlapped branch was always welded to the chord, and the remainder of the welds in the truss were sized so as to not fail before yielding of the attached branch member. Figure 3 shows the specified weld sizes and the associated welding symbols in a typical connection detail for a joint with  $O_v = 30\%$ .

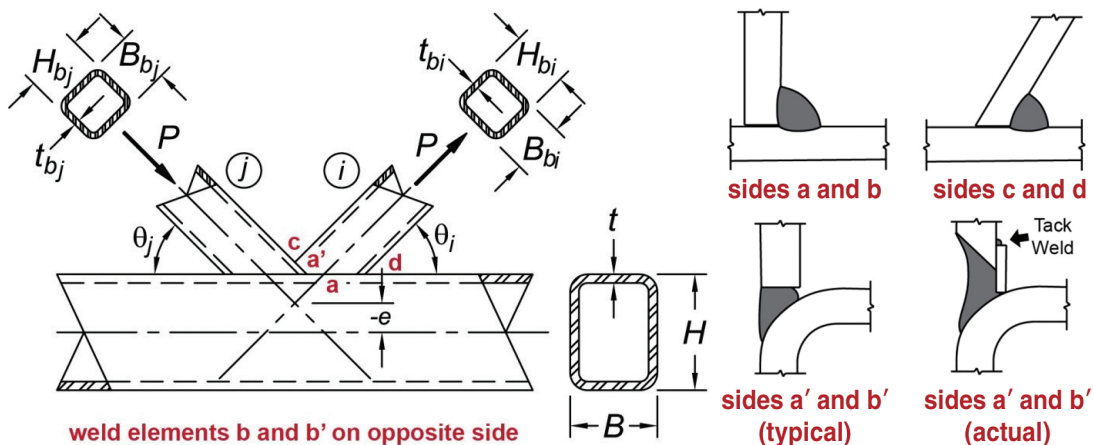


Fig. 2. Terminology for HSS K-connections and weld details (including labeling convention) for test joints.

During fabrication, the backing bar in detail a' of K-60-0.50 was pried about the tack weld (see Figure 2), away from the inside face of the HSS branch. The member itself was the last one to be fitted into the truss and was hammered into place. It is believed that during hammering, the backing bar—which made contact with the chord—was caught, causing it to be pried. This complication was not identified until after welding of the opposite side (details b and b') was complete. The resulting “gap” was filled with weld metal and welding of the test joint proceeded. Based on nondestructive test (NDT) results, this was not a cause for rejection; however, it is speculated that the strength of the joint was nevertheless affected by this defect. The joint is identified in the subsequent analysis (Figures 11 through 16) by a red data point.

All of the test welds were ground (long after welding) to reduce the weld throat dimension to below the minimum sizes specified by AISC and AWS. This was necessary to obtain a weld-fracture failure mode. Because the code provisions are based on achieving the necessary heat input at

the time of welding, and because minimum sizes were at that time provided, the soundness of the welds was likely unaffected.

## MATERIAL GEOMETRIC AND MECHANICAL PROPERTIES

The measured geometric and mechanical properties of the HSS members and the nine test connections are shown in Table 1.

For the PJP welds, the throat dimension ( $t_w$ ) of the PJP flare-bevel-groove welds (side a') was measured according to Equation 1:

$$t_w = t_{bi} - d \quad (1)$$

where  $d$  is the greatest perpendicular dimension measured from a line flush to the overlapping branch member surface to the weld surface and  $t_{bi}$  is the average measured thickness of the overlapping branch member.

For the fillet welds,  $t_w$  was determined by making a negative mold of each fillet weld element at numerous locations along its length. The mold was cut normal to the axis of the weld root, scanned and digitally measured; the effective throat was taken as the minimum distance between the root and face of the diagrammatic weld. Figure 4 shows a cut of the mold and a typical weld throat measurement.

More than 180 weld dimensions were taken for the nine connections (five along each of the four sides of the connection), and the average measured values for the weld throat dimension are shown in Table 2.

Mechanical properties of the as-laid welds were determined by tensile coupon tests (three total) as specified by AWS D1.1 (2010). The results are shown in Table 3. The average yield stress (by 0.2% strain offset) was 81.6 ksi, and the average ultimate strength ( $F_{EXX}$ ) was 89.8 ksi with 27.5% elongation at rupture. The measured ultimate strength was 28% stronger than the nominal strength of the electrode used (AWS E71T-1C).

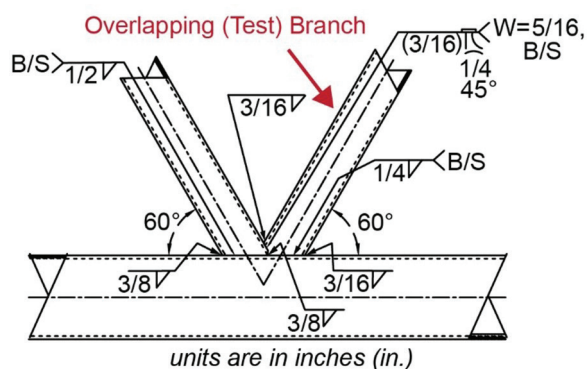


Fig. 3. Typical connection detail drawing (connection K-30-0.50a or K-30-0.50b).

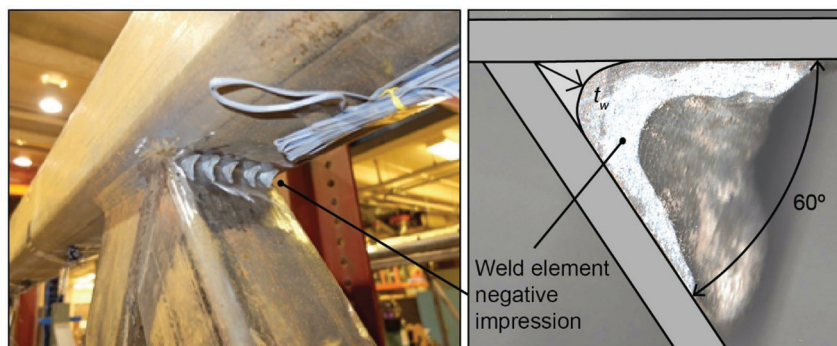


Fig. 4. Typical measurement procedure and mold profile.

Table 2. Average Effective Weld Throat Thickness for Individual Weld Elements						
Test	Measured Weld Throat Dimension, in.					
	a	a'	b	b'	c	d
K-90-0.50a	0.136	0.125	0.123	0.141	0.148	0.168
K-90-0.50b	0.181	0.136	0.150	0.144	0.151	0.168
K-60-0.50	0.105	0.150	0.094	0.140	0.152	0.166
K-30-0.50a	0.132	0.181	0.116	0.156	0.171	0.143
K-30-0.50b	0.129	0.169	0.120	0.169	0.158	0.139
K-90-0.71	0.125	0.153	0.125	0.150	0.143	0.151
K-60-0.71a	0.157	0.138	0.152	0.123	0.149	0.152
K-60-0.71b	0.135	0.140	0.127	0.148	0.151	0.156
K-30-0.71	0.180	0.194	0.134	0.188	0.168	0.149
T2 Joint 4 <sup>†</sup>	0.177	0.177	0.173	0.173	0.283	0.264
T2 Joint 6 <sup>†</sup>	0.280	0.280	0.256	0.256	0.358	0.417

Note: b and b' are analogous to a and a' (see Figure 2), but on the opposite side of the overlapping branch.

Table 3. All-Weld-Metal Tensile Coupon Test Results				
All-Weld-Metal Coupon Designation	$F_y$ , ksi	$E \times 10^3$ ksi	$F_{EXX}$ , ksi	$\epsilon_{rup}$ , %
[i]	81.0	29.3	91.2	27.0
[ii]	81.4	29.0	88.7	26.4
[iii]	82.3	31.8	89.5	29.2
<b>Average</b>	<b>81.6</b>	<b>30.0</b>	<b>89.8</b>	<b>27.5</b>

## INSTRUMENTATION AND LOADING STRATEGY

### Instrumentation

The actual weld fracture loads ( $P_d$ ) were obtained from two linear strain gages (SGs) located in-plane and at mid-length (in the constant elastic stress region) of the web members (Mehrota and Govil, 1972). The breaking loads were hence calculated according to Equation 2:

$$P_d = A_b E \epsilon_{avg} \quad (2)$$

where

$A_b$  = cross-sectional area of the branch, determined by weighing the cross-section

$E$  = elastic modulus of the rectangular HSS, determined by tensile coupon tests in accordance with ASTM A370 (ASTM, 2009)

$\epsilon_{avg}$  = average strain measured on opposite faces of the rectangular HSS

The nonuniform normal strain distribution around the branch perimeter, adjacent to the weld, was measured using SGs oriented along the longitudinal axis of the member and

1 in. away from the weld toe [in order to avoid the strain concentrations caused by the notch effect (Packer and Cassidy, 1995)]. Because the strain distribution is theoretically symmetric about the  $y$ - $y$  axis of the member (for plane-frame behavior), SGs were only installed on half of the member (along  $H_{bi}$  and half of  $B_{bi}$  on two sides). The SG spacing is shown in Figure 5.

### Loading Strategy

The single-point load was applied at a truss panel point by a 600-kip capacity MTS Universal Testing Frame and resulted, by design, in a distribution of member forces that accentuated the load in a particular, predetermined branch member (ergo, the weld to it). Failure was planned to always occur in the test welds, instead of by some connection, member or stability failure mode.

After rupture occurred in the intended test weld, the connection was repaired by overwelding the gap with a new weld designed to develop the yield strength of the member. Hence, the welded connection was no longer critical. The location of the point load was subsequently altered to cause

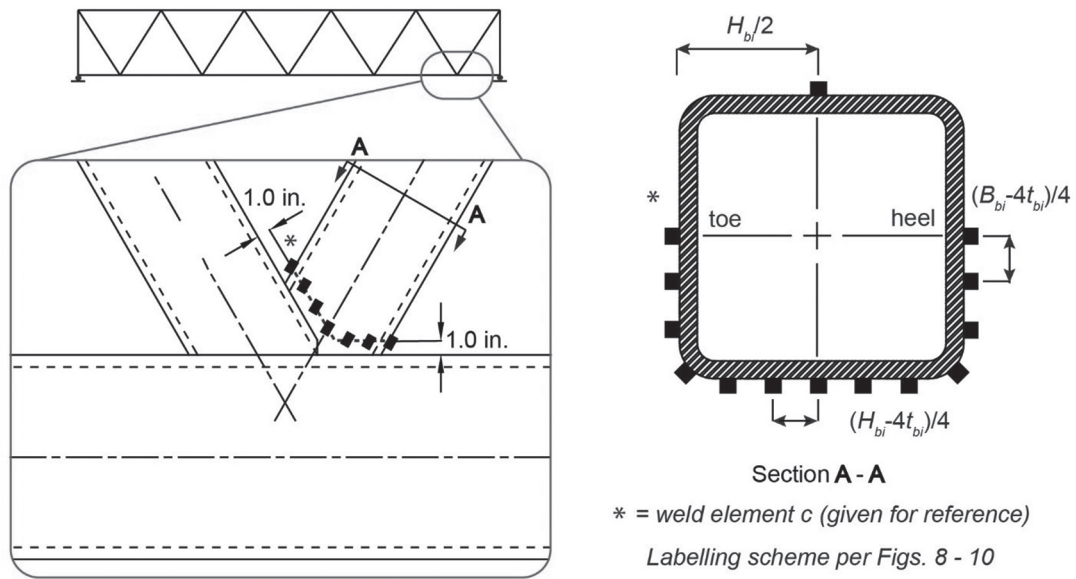


Fig. 5. Spacing of strain gages around the branch footprint adjacent to the welded connection.

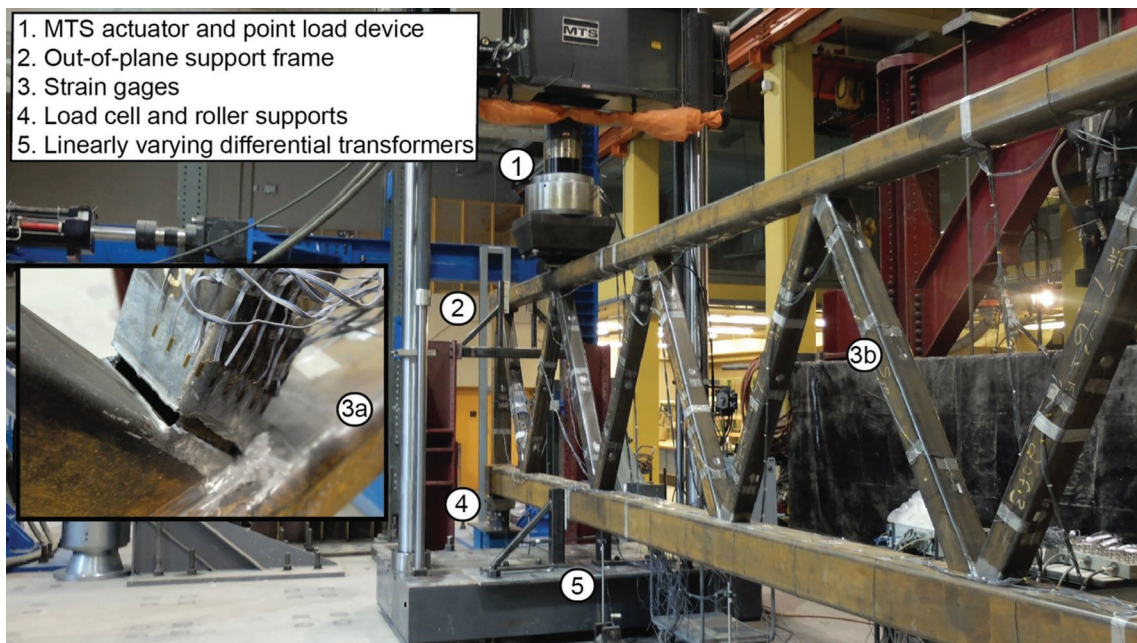


Fig. 6. Laboratory testing arrangement for full-scale HSS overlapped K-connection experiments.

failure at another joint. Because the MTS test frame was fixed to the laboratory floor, the truss itself was either translated, rotated 180 degrees and/or inverted to achieve the new distribution of forces. The roller supports were always located at the ends of the truss, as seen in Figure 1.

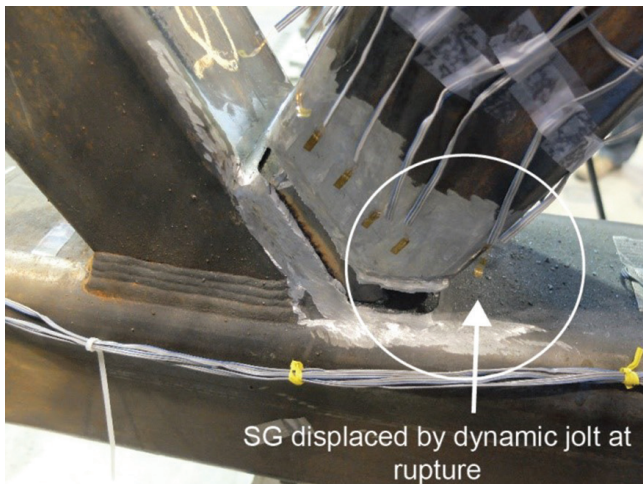
The laboratory testing arrangement and a series of typical weld fractures are shown in Figures 6 and 7, respectively.

## RESULTS

All of the test welds failed in a brittle manner by fracture along a plane through the weld, which occurred simultaneously at all locations around the branch perimeter. Failure was sudden and accompanied by a dynamic “jolt” (caused by the release of strain energy) that, in some tests, displaced SGs from the branch member surface (see Figure 7a).

Figure 8 shows the relationship between the applied MTS load and the load in the branch member (measured by SGs in the position shown) for test K-30-0.50a. By virtue of a constant slope (indicating a linear variation in average strain), it can be seen that the member itself remained elastic throughout the entire load range. The branch load at rupture was hence calculated using Equation 2.

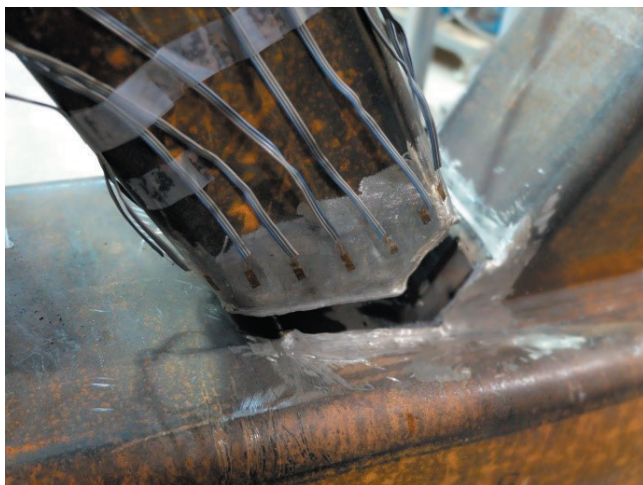
Figures 9, 10 and 11 show the variation in strain measured at 13 different SGs adjacent to the test welds at the initial unloaded stage and at 50%, 80% and 100% of the weld rupture load. For the joints tested, it was found that the magnitude of strain decreased as a function of the distance from the toe of the connection—believed to be caused by differences in the relative stiffness of the chord ( $\beta = 0.50$  and  $B/t = 27.5$ ) and the overlapped branch ( $\beta = 1.00$  and  $B_{bj}/t_{bj} = 16.3$ ) that results in the latter attracting more load.



(a) Test K-60-0.71a



(b) Test K-30-0.50a



(c) Test K-30-0.50b



(d) Test K-90-0.71

Fig. 7. Typical weld fractures and instrumentation.

As  $O_v$  increases, this change becomes less pronounced and is accompanied, generally, by a higher average failure stress in the weld. The magnitude of strain along the branch transverse faces is seen to decrease toward the mid-wall locations (SGs 1 and 13) except for the final stage of stress redistribution (Figures 9 and 11). This variation is expectedly more pronounced when the branch lands on a flexible chord ( $\beta = 0.50$ ,  $B/t = 27.5$ ) and for low values of  $O_v$ . The less sudden change in strain approaching the mid-wall along the toe (in Figures 9–11) is due to the more uniform transverse stiffness of the overlapped branch ( $\beta = 1.00$  and  $B/t = 16.3$ ).

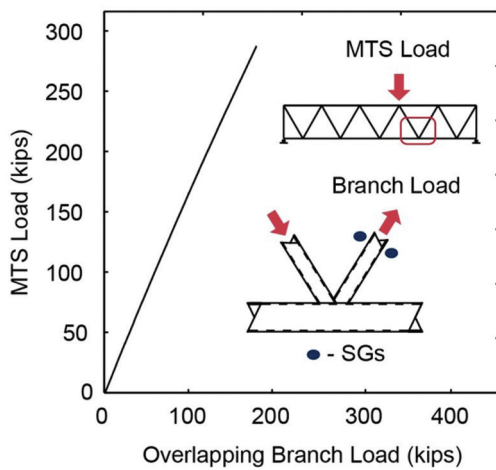


Fig. 8. MTS load versus branch load magnitude relationship (test K-30-0.50a).

In Figure 9, much of the weld to the heel actually remains in compression for the entire load range (branch in tension). The high strain at the toe in Figure 9 may be caused by the proximity of the transverse weld to the hidden toe of the overlapped branch, which was itself welded and thus increased the stiffness of the connection and the weld effective length at this location.

The distributions of strain around the branch members adjacent to the test welds shows that longitudinal welds to overlapped K-connections can be regarded as completely effective at resisting the applied load when  $O_v = 60\%$  and  $90\%$ . For  $O_v = 30\%$  (Figure 9), the strain along the longitudinal weld (SGs 4–10) can be seen to be more nonuniform. The transverse welds are always only partially effective and generally become less effective as the  $\beta$ -ratio decreases, as  $O_v$  decreases and as  $B/t$  increases. These trends are verified by the actual rupture loads ( $P_a$ ) given in Table 4. They are generally in accordance with predictions given by the existing AISC Specification (AISC, 2010) formulas (Equations 4–8).

### EVALUATION OF AISC 360-10

#### Existing Provisions for Weld Effective Lengths in Rectangular HSS Overlapped K-Connections

According to the Load and Resistance Factor Design (LRFD) method of AISC 360 (2010), the available strength of welds to axially loaded rectangular HSS branches ( $P_{mw}$ ) is based on the limit state of shear rupture along the plane of the weld effective throat, according to Equation 3:

$$P_{mw} = F_{mw} t_w l_e \quad (3)$$

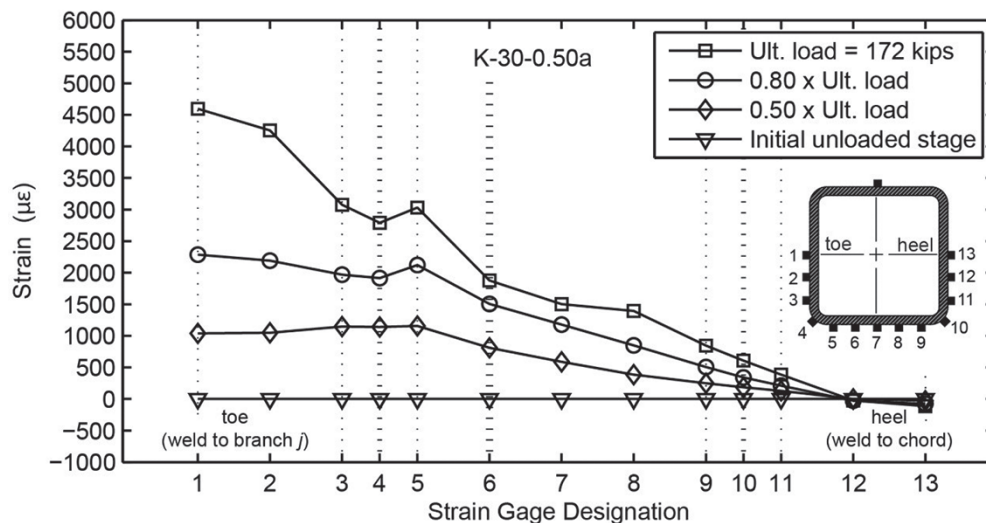


Fig. 9. Typical distribution of normal strain around branch perimeter for specimens with  $O_v = 30\%$ ,  $\beta = 0.50$  and  $B/t = 27.5$ .

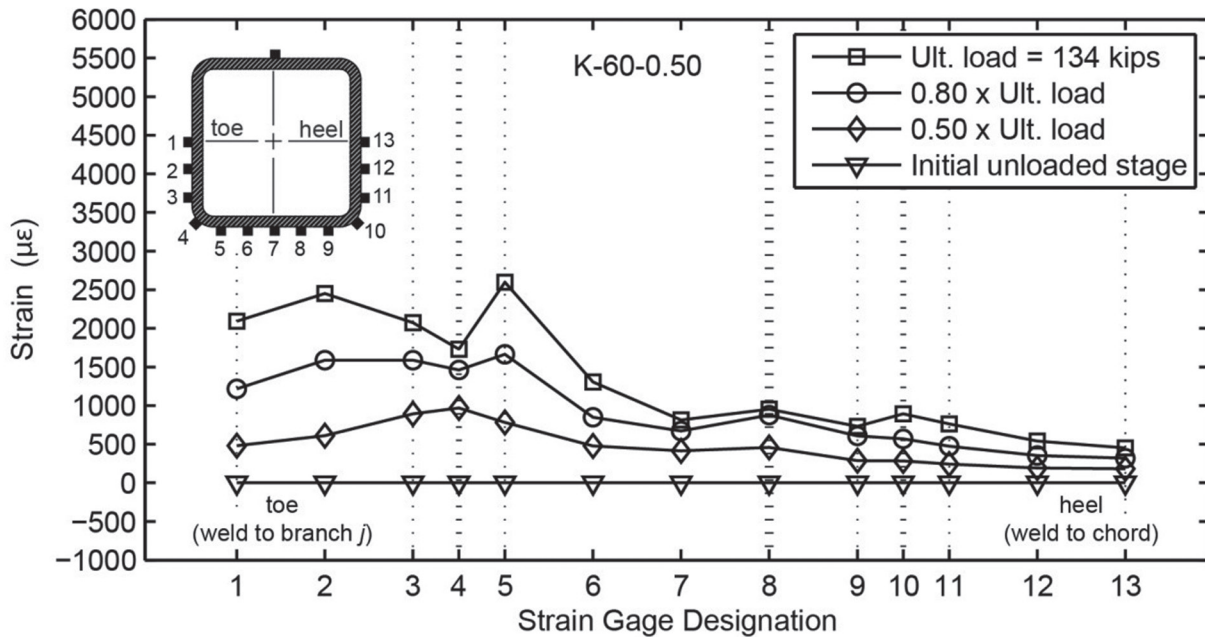


Fig. 10. Typical distribution of normal strain around branch perimeter for specimens with  $O_v = 60\%$ ,  $\beta = 0.50$  and  $B/t = 27.5$ .

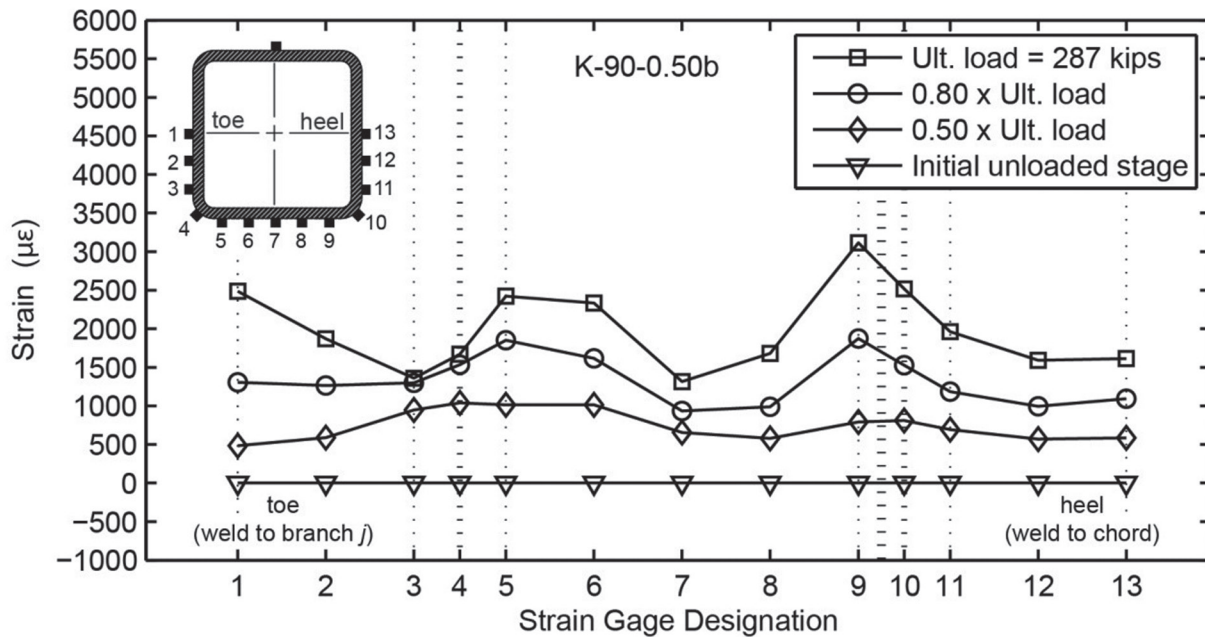


Fig. 11. Typical distribution of normal strain around branch perimeter for specimens with  $O_v = 90\%$ ,  $\beta = 0.50$  and  $B/t = 27.5$ .

**Table 4. Actual and Predicted Nominal Weld Strength for Each Test Connection**

Test	$P_a^{**}$	$P_{nw}$		
	kips	Current AISC 360-10 kips	Modified AISC 360-10 kips	Without Weld Effective Lengths kips
K-90-0.50a	277	187	197	217
K-90-0.50b	287	196	206	227
K-60-0.50*	134	138	154	201
K-30-0.50a	172	86	102	191
K-30-0.50b	166	85	101	187
K-90-0.71	256	199	209	228
K-60-0.71a	219	146	160	201
K-60-0.71b	194	149	163	205
K-30-0.71	237	104	119	213
T2 Joint 4 <sup>†</sup>	379	175	192	257
T2 Joint 6 <sup>†</sup>	375	262	286	378

Note: Italicized values are strength predictions that exceed the measured strength (i.e., nominally unsafe).

\* Imperfect weld root detail (see "Weld Joint Details").

\*\* Force in overlapping web member at weld fracture.

† Tests by Frater (1991); failed by a combined mechanism of weld fracture and premature branch yielding.

where

$F_{nw}$  = nominal strength of weld metal

$t_w$  = weld effective throat around the perimeter of the branch

$l_e$  = effective length of fillet and groove welds.

An LRFD resistance factor,  $\phi$ , equal to 0.75 and 0.80, applies for fillet welds and PJP groove welds, respectively.

In Table J2.5 of AISC 360-10,  $F_{nw}$  is specified as  $0.60F_{EXX}$  for both fillet and PJP groove welds. In the case of the former, it implies that the failure mode is by shear rupture on the effective throat; however, for PJP groove welds (sides a' and b'), it is an arbitrary reduction factor that has been in effect since the early 1960s to compensate for the notch effect of the unfused area of the joint and does not imply that the tensile failure mode is by shear stress on the effective throat (per AISC 360-10 Commentary to Chapter J). Because a CP detail was provided (see "Weld Joint Details") in order to establish a high degree of certainty with respect to the fusion area (and the weld throat dimension) in this region, a more suitable term of  $1.00F_{EXX}$  has been used herein for  $F_{nw}$  for groove welds.

The formulas for  $l_e$  are given in Table K4.1 of AISC 360 and are as follows:

- When  $25\% \leq O_v < 50\%$ :

$$l_{e,i} = \frac{20_v}{50} \left[ \left( 1 - \frac{O_v}{100} \right) \left( \frac{H_{bi}}{\sin \theta_i} \right) + \frac{O_v}{100} \left( \frac{H_{bi}}{\sin(\theta_i + \theta_j)} \right) \right] + b_{eoi} + b_{eov} \quad (4)$$

- When  $50\% \leq O_v < 80\%$ :

$$l_{e,i} = 2 \left[ \left( 1 - \frac{O_v}{100} \right) \left( \frac{H_{bi}}{\sin \theta_i} \right) + \frac{O_v}{100} \left( \frac{H_{bi}}{\sin(\theta_i + \theta_j)} \right) \right] + b_{eoi} + b_{eov} \quad (5)$$

- When  $80\% \leq O_v \leq 100\%$ :

$$l_{e,i} = 2 \left[ \left( 1 - \frac{O_v}{100} \right) \left( \frac{H_{bi}}{\sin \theta_i} \right) + \frac{O_v}{100} \left( \frac{H_{bi}}{\sin(\theta_i + \theta_j)} \right) \right] + B_{bi} + b_{eov} \quad (6)$$

where

$i$  = subscript used to refer to the overlapping branch

$j$  = subscript used to refer to the overlapped branch

$H_b$  = overall height of the branch member measured in the plane of the connection

$\theta$  = included angle between the branch and the chord  
=  $60^\circ$  for all test connections

The total weld effective length is shown in Figure 12.

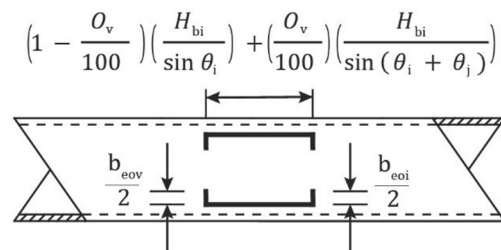


Fig. 12. Weld effective length dimensions.

The terms  $b_{eoi}$  and  $b_{eov}$  are empirically derived from laboratory tests (Davies and Packer, 1982) and quantify the effective widths of weld to the branch face, normal (transverse) to the plane of the connection:

$$b_{eoi} = \frac{10}{B/t} \left( \frac{F_y t}{F_{ybi} t_{bi}} \right) B_{bi} \leq B_{bi} \quad (7)$$

$$b_{eov} = \frac{10}{B_{bj}/t_{bj}} \left( \frac{F_{ybj} t_{bj}}{F_{ybi} t_{bi}} \right) B_{bi} \leq B_{bi} \quad (8)$$

where

$B$  = overall width of the chord, normal to the plane of the connection

$B_b$  = overall width of the branch, normal to the plane of the connection

$t$  = wall thicknesses of the chord

$t_b$  = wall thicknesses of the branch

$F_y$  = yield stress of the chord

$F_{yb}$  = yield stress of the branch

AISC 360 also currently limits the values of  $b_{eoi}/2$  and  $b_{eov}/2$  through a notwithstanding clause, which states,

When  $B_{bi}/B > 0.85$  or  $\theta_i > 50^\circ$ ,  $b_{eoi}/2$  shall not exceed  $2t$  and when  $B_{bi}/B_{bj} > 0.85$  or  $(180^\circ - \theta_i - \theta_j) > 50^\circ$ ,  $b_{eov}/2$  shall not exceed  $2t_{bj}$ .

Thus, for the HSS overlapped K-connections tested, the upper limits of  $b_{eoi} = 4t$  and  $b_{eov} = 4t_{bj}$  apply.

### Safety Level Implicit in AISC 360

In order to assess whether adequate or excessive safety margins are inherent, one can check to ensure that a minimum safety index ( $\beta+$ ) of 4.0, as currently adopted by AISC 360-10 per Chapter B of the *Specification Commentary* (AISC, 2010), is achieved using a simplified reliability analysis in which  $\phi$  is given by Equation 9 (Fisher et al., 1978; Ravindra and Galambos, 1978):

$$\phi = m_R \cdot \exp(-\alpha\beta^+ COV) \quad (9)$$

where

$m_R$  = mean of the ratio of actual element strength to predicted nominal element strength

$COV$  = associated coefficient of variation of the ratio of actual element strength to predicted nominal element strength

$\alpha$  = coefficient of separation taken to be 0.55 (Ravindra and Galambos, 1978)

In the evaluation that follows, correlation plots are produced using the measured ultimate weld strengths (rupture loads) from the nine tests and the results from two similar

connection tests that were conducted at the University of Toronto, the details of which appear at the bottom of Table 1 (Frater and Packer, 1992a, 1992b).

The implied resistance factor,  $\phi$ , is equal to 0.922 for the existing AISC *Specification* provisions and is larger than the necessary resistance factors for fillet welds and PJP groove welds (0.75 and 0.80, respectively), indicating an excessive level of safety for the current AISC formulas. Figure 13 shows the correlation of the predicted nominal strengths with the experimental results.

## RECOMMENDATION

### Background

By means of 12 full-scale experiments on isolated T-connections, conducted during phase 1 of the research program, excessive safety was found to exist in the current AISC 360 (2010) formula for the effective elastic section modulus for in-plane bending for rectangular HSS moment T-connections (McFadden and Packer, 2014). The authors proposed a change to the current requirement that restricts the effective widths of welds to the branch face from two times the chord wall thickness ( $2t$ ) to a more reasonable limit of  $B_b/4$ .

Their proposal increases the effective length of the transverse weld elements in most rectangular HSS connections and was shown to also be applicable to the formulas for the effective length of welds in axially loaded rectangular HSS T- and X- (or cross-) connections.

### Proposal

Because the same pattern is observed for rectangular HSS overlapped K-connections, it is proposed that the existing formulas for the effective length of welds be modified in the same manner, by changing the requirement,

When  $B_{bi}/B > 0.85$  or  $\theta_i > 50^\circ$ ,  $b_{eoi}/2$  shall not exceed  $2t$  and when  $B_{bi}/B_{bj} > 0.85$  or  $(180^\circ - \theta_i - \theta_j) > 50^\circ$ ,  $b_{eov}/2$  shall not exceed  $2t_{bj}$ .

to

When  $B_{bi}/B > 0.85$  or  $\theta_i > 50^\circ$ ,  $b_{eoi}/2$  shall not exceed  $B_{bi}/4$  and when  $B_{bi}/B_{bj} > 0.85$  or  $(180^\circ - \theta_i - \theta_j) > 50^\circ$ ,  $b_{eov}/2$  shall not exceed  $B_{bi}/4$ .

This change produces the correlation with the test data given by Figure 14.

### Safety Level Implicit in Recommendation

The implied resistance factor,  $\phi$ , is equal to 0.875 for the recommended modification to the existing AISC *Specification* provisions (AISC, 2010), which is still larger than the necessary resistance factors for fillet welds and PJP groove

welds. More importantly, using these modified AISC provisions for rectangular HSS overlapped K-connections results in consistency for the aggregate recommended design rules for welds in rectangular HSS connections, including axially loaded rectangular HSS T- and X- (or cross-) connections, moment T-connections and overlapped K-connections.

### Comments

It is worth noting that if no effective length rules are applied, and if the total weld length is used to determine the strength of the welded joint to the overlapping branch, then the correlation with the test data shown in Figure 13 results. The implied resistance factor,  $\phi$ , is equal to 0.674, which is less than the necessary resistance factors for fillet and PJP welds, illustrating that such an approach provides an insufficient safety margin. If historical tests (Frater, 1991) are omitted from the analysis, a marginal reduction to the inherent safety factors is found; however, the previous discussion still applies, and the recommendation is found to be safe. Correlations to this effect are given in Figures 16, 17 and 18.

If the hidden toe of the overlapped branch was not welded, a smaller effective length may result at the toe of the overlapping branch ( $b_{eov}$ ) because the restraint to transverse deformation (stiffness) would be less. This would tend to reduce the mean of the actual element strength to predicted nominal element strength ( $m_R$ ) in Equation 9; however, by virtue of  $m_R$  being already higher for connections with  $O_v =$

30% relative to the other connections, there would be some counteracting decrease in  $COV$ , and thus a minimal effect on the reliability of the proposed changes.

### CONCLUSIONS

Based on the results from nine full-scale tests on weld-critical rectangular HSS-to-HSS overlapped K-connections and the measured strength of two overlapped K-connection tests from a previous experimental program (Frater, 1991), it has been found that:

- The distribution of normal strain adjacent to the welded joint in rectangular HSS overlapped K-connections is highly nonuniform.
- As the overlap increases, stiffening the joint, the distribution of normal strain adjacent to the welded joint becomes more uniform.
- Transverse welds are only partially effective and generally become less effective as the  $\beta$ -ratio decreases, as  $O_v$  decreases and as  $B/t$  (of the landing surface) increases.
- The current effective length rules defined by Equations K4-10, K4-11 and K4-12 and given in Table K4.1 of AISC 360 (2010) for welds in rectangular HSS-to-HSS overlapped K-connections are quite conservative.

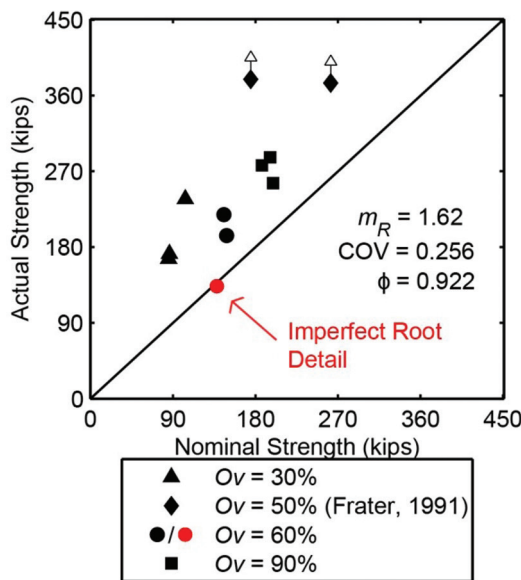


Fig. 13. Correlation with all test results for current AISC 360-10 provisions.

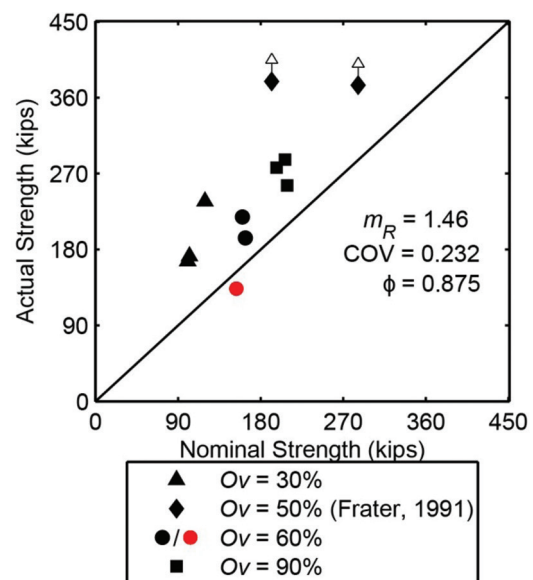


Fig. 14. Correlation with all test results for modified AISC 360-10 provisions.

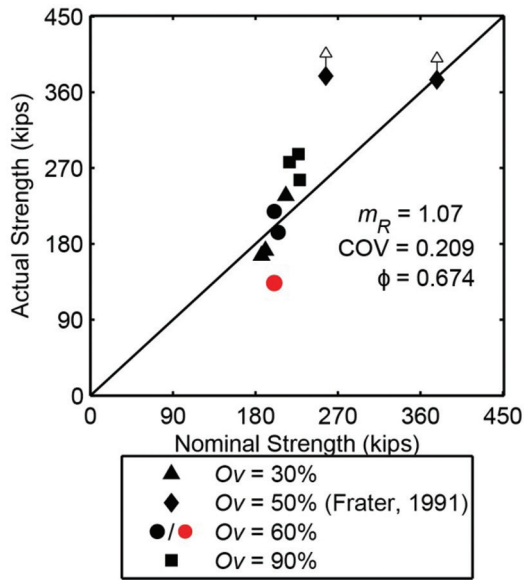


Fig. 15. Correlation with all test results not using effective length rules.

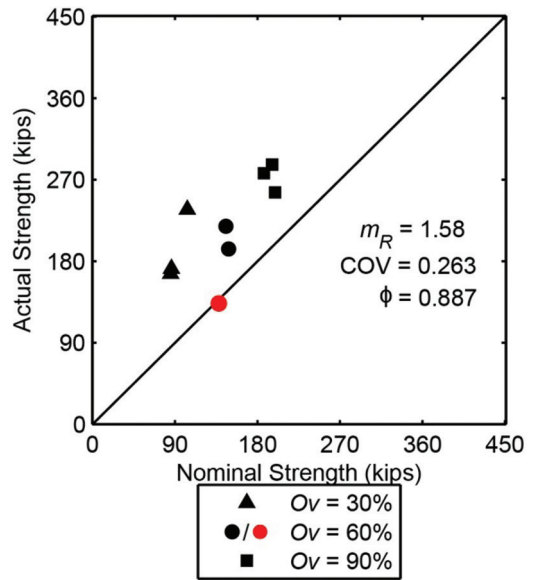


Fig. 16. Correlation with current test results for current AISC 360-10 provisions.

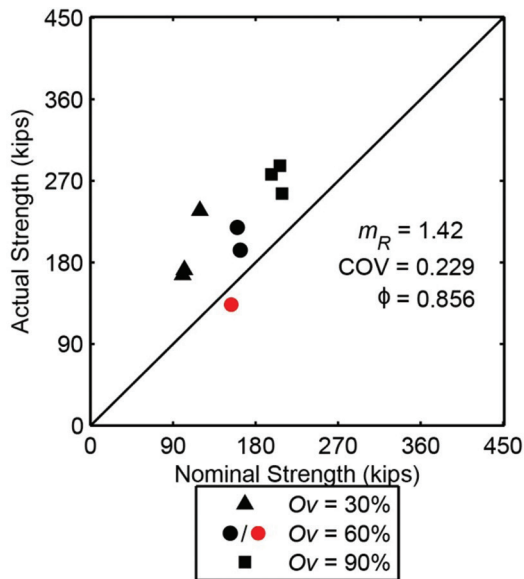


Fig. 17. Correlation with current test results for modified AISC 360-10 provisions.

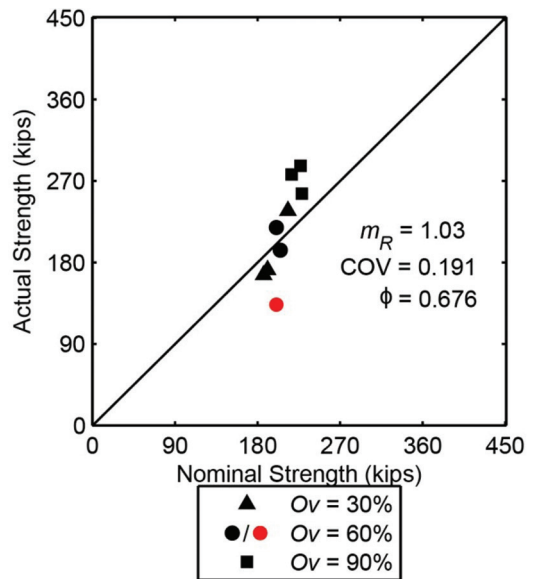


Fig. 18. Correlation with current test results without using weld effective length rules.

## RECOMMENDATION

It is recommended to modify the requirement (AISC 360-10)

When  $B_{bi}/B > 0.85$  or  $\theta_i > 50^\circ$ ,  $b_{eoi}/2$  shall not exceed  $2t$  and when  $B_{bi}/B_{bj} > 0.85$  or  $(180^\circ - \theta_i - \theta_j) > 50^\circ$ ,  $b_{eov}/2$  shall not exceed  $2t_{bj}$ .

to

When  $B_{bi}/B > 0.85$  or  $\theta_i > 50^\circ$ ,  $b_{eoi}/2$  shall not exceed  $B_{bi}/4$  and when  $B_{bi}/B_{bj} > 0.85$  or  $(180^\circ - \theta_i - \theta_j) > 50^\circ$ ,  $b_{eov}/2$  shall not exceed  $B_{bi}/4$ .

to increase the predicted strength of welded joints in rectangular HSS overlapped K-connections. This modification is adopted from McFadden and Packer (2014) and has been shown to still be conservative yet generally provide a more economical design approach for rectangular HSS T-, Y- and X- (or cross-) connections subject to branch axial load or branch bending. Using this recommendation would thus establish consistent rules across AISC 360 for the design of welded truss connections between HSS.

## DESIGN EXAMPLE

### Given:

A planar roof truss contains the welded HSS 60-degree overlapped K-connection shown in Figure 19. Note that the chord moment is necessary for equilibrium because of the nodding eccentricity. The connection is a balanced K-connection because the vertical component of the compression branch member force is equilibrated (within 20%) by the vertical component of the tension branch member force [see AISC 360-10, Section K2(b)]. The through branch is the wider and thicker branch member. For fabrication, the compression (through) branch is fully welded (overlapped/hidden toe included) to the chord, the diagonal (overlapping) branch is then tacked into place and finally the whole connection is welded together. The loads shown consist of live load and dead load in the ratio of 3:1. Determine the adequacy of the connection under the given loads, and the required weld throat, for each of the branches, using the effective length approach. Assume matched electrodes with a specified ultimate strength of 70 ksi.

From AISC *Manual* Table 2-3 (AISC, 2011), the HSS material properties are as follows:

#### All members

ASTM A500 Grade B

$$F_y = F_{yb} \\ = 46 \text{ ksi}$$

$$F_u = F_{ub} \\ = 58 \text{ ksi}$$

#### Weld consumable

$$F_{EXX} = 70 \text{ ksi}$$

From AISC *Manual* Tables 1-11 and 1-12, the HSS geometric properties are as follows:

$$\begin{aligned} \text{HSS}8 \times 8 \times \frac{1}{2} \\ A &= 13.5 \text{ in.}^2 \\ B &= 8.00 \text{ in.} \\ H &= 8.00 \text{ in.} \\ t &= 0.465 \text{ in.} \end{aligned}$$

$$\begin{aligned} \text{HSS}6 \times 4 \times \frac{5}{16} \\ A_{bj} &= 5.26 \text{ in.}^2 \\ B_{bj} &= 4.00 \text{ in.} \\ H_{bj} &= 6.00 \text{ in.} \\ t_{bj} &= 0.291 \text{ in.} \end{aligned}$$

$$\begin{aligned} \text{HSS}5 \times 3 \times \frac{1}{4} \\ A_{bi} &= 3.37 \text{ in.}^2 \\ B_{bi} &= 3.00 \text{ in.} \\ H_{bi} &= 5.00 \text{ in.} \\ t_{bi} &= 0.233 \text{ in.} \end{aligned}$$

### Solution:

#### *Limits of Applicability*

Check the limits of applicability for rectangular HSS given in AISC *Specification* Section K2.3 (AISC, 2010). Connection nodding eccentricity,  $e = -1.00$  in. (negative because the branch centerlines intersect toward the branches, relative to the chord centerline).

$q$  = overlap length measured along the connecting face of the chord beneath the two branches, from geometry

$$= \left( \frac{H_{bj}}{2\sin \theta_{bj}} + \frac{H_{bi}}{2\sin \theta_{bi}} \right) - \left( \frac{e + H/2}{\frac{\sin \theta_{bj} \sin \theta_{bi}}{\sin(\theta_{bj} + \theta_{bi})}} \right)$$

$$= \left( \frac{6.00 \text{ in.}}{2\sin 60^\circ} + \frac{5.00 \text{ in.}}{2\sin 60^\circ} \right) - \left( \frac{-1.00 \text{ in.} + 4.00 \text{ in.}}{\frac{(\sin 60^\circ)^2}{\sin 120^\circ}} \right)$$

$$= 6.35 \text{ in.} - 3.46 \text{ in.}$$

$$= 2.89 \text{ in.}$$

$p$  = projected length of the overlapping branch on the chord

$$= \frac{5.00 \text{ in.}}{\sin 60^\circ}$$

$$= 5.77 \text{ in.}$$

$$O_v = \left( \frac{q}{p} \right) (100\%)$$

$$= \left( \frac{2.89}{5.77} \right) (100\%)$$

$$= 50\%$$

$$-0.55 \leq \frac{e}{H} = -0.125 \leq 0.25 \quad \text{o.k.}$$

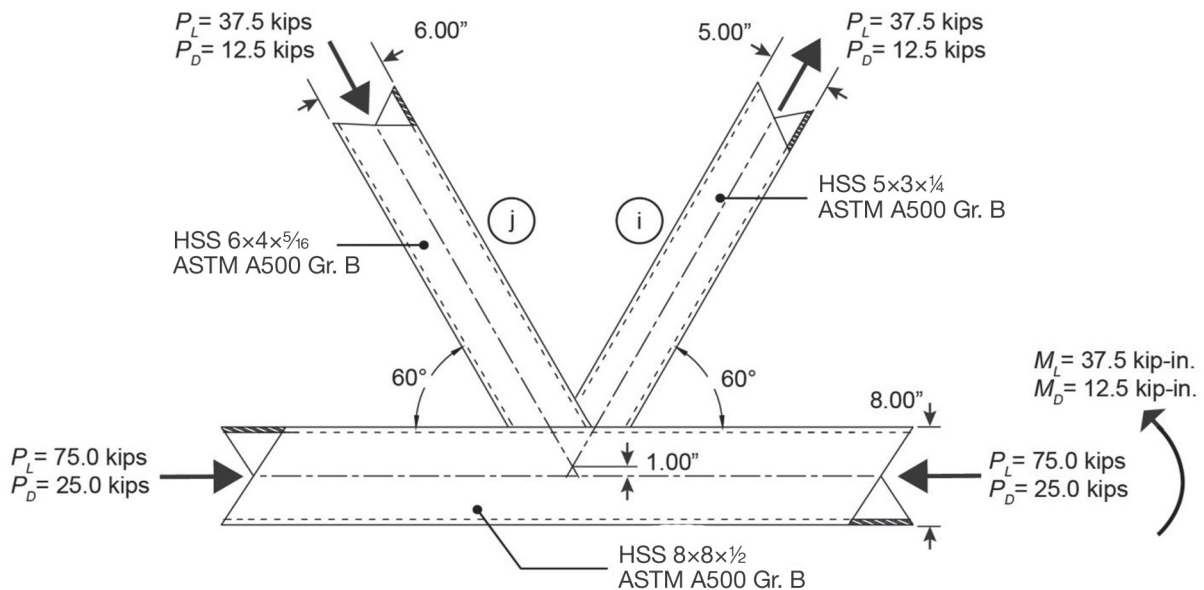


Fig. 19. Welded overlapped K-connection with rectangular HSS.

As the nodding eccentricity satisfied this limit, the resulting total eccentricity moment that it produces [(2(1.00 in.)(50 kips) (cos 60°) = 50 kip-in.] can be neglected with regard to connection design. (However, it would still have an effect on chord member design in general).

$$\theta_{bi} = \theta_{bj}$$

$$= 60^\circ \geq 30^\circ \quad \mathbf{o.k.}$$

$$\frac{B}{t} = \frac{8.00 \text{ in.}}{0.465 \text{ in.}}$$

$$= 17.2 \leq 30 \quad \mathbf{o.k.}$$

$$\frac{H}{t} = \frac{8.00 \text{ in.}}{0.465 \text{ in.}}$$

$$= 17.2 \leq 35 \quad \mathbf{o.k.}$$

For the tension branch:

$$\frac{B_{bi}}{t_{bi}} = \frac{3.00 \text{ in.}}{0.233 \text{ in.}}$$

$$= 12.9 \leq 35 \quad \mathbf{o.k.}$$

$$\frac{H_{bi}}{t_{bi}} = \frac{5.00 \text{ in.}}{0.233 \text{ in.}}$$

$$= 21.5 \leq 35 \quad \mathbf{o.k.}$$

For the compression branch:

$$\frac{B_{bj}}{t_{bj}} = \frac{4.00 \text{ in.}}{0.291 \text{ in.}}$$

$$= 13.7 \leq 1.1 \sqrt{\frac{E}{F_{yb}}} = 1.1 \sqrt{\frac{29,000}{46 \text{ ksi}}} = 27.6$$

$$13.7 \leq 27.6 \quad \mathbf{o.k.}$$

$$\frac{H_{bj}}{t_{bj}} = \frac{6.00 \text{ in.}}{0.291 \text{ in.}}$$

$$= 20.6 \leq 1.1 \sqrt{\frac{E}{F_{yb}}}$$

$$20.6 \leq 27.6 \quad \mathbf{o.k.}$$

For the tension branch:

$$\frac{B_{bi}}{B} = \frac{3.00 \text{ in.}}{8.00 \text{ in.}}$$

$$= 0.375 \geq 0.25 \quad \mathbf{o.k.}$$

$$\frac{H_{bi}}{B} = \frac{5.00 \text{ in.}}{8.00 \text{ in.}}$$

$$= 0.625 \geq 0.25 \quad \mathbf{o.k.}$$

For the compression branch:

$$\begin{aligned}\frac{B_{bj}}{B} &= \frac{4.00 \text{ in.}}{8.00 \text{ in.}} \\ &= 0.500 \geq 0.25 \quad \mathbf{o.k.} \\ \frac{H_{bj}}{B} &= \frac{6.00 \text{ in.}}{8.00 \text{ in.}} \\ &= 0.750 \geq 0.25 \quad \mathbf{o.k.}\end{aligned}$$

For the tension branch:

$$\begin{aligned}0.5 &\leq \frac{H_{bi}}{B_{bi}} \leq 2.0 \\ \frac{H_{bi}}{B_{bi}} &= \frac{5.00 \text{ in.}}{3.00 \text{ in.}} \\ &= 1.67 \\ 0.5 &\leq 1.67 \leq 2.0 \quad \mathbf{o.k.}\end{aligned}$$

For the compression branch:

$$\begin{aligned}0.5 &\leq \frac{H_{bj}}{B_{bj}} \leq 2.0 \\ \frac{H_{bj}}{B_{bj}} &= \frac{6.00 \text{ in.}}{4.00 \text{ in.}} \\ &= 1.50 \\ 0.5 &\leq 1.50 \leq 2.0 \quad \mathbf{o.k.}\end{aligned}$$

For the chord:

$$\begin{aligned}0.5 &\leq \frac{H}{B} = 1.00 \leq 2.00 \quad \mathbf{o.k.} \\ 25\% &\leq O_v = 66.7\% \leq 100\% \quad \mathbf{o.k.}\end{aligned}$$

The width of the overlapping branch,  $B_{bi}$ , divided by the width of the overlapped branch,  $B_{bj}$ , must be greater than or equal to 0.75, where  $B_{bi}$  and  $B_{bj}$  are the branch widths perpendicular to the longitudinal axis of the chord.

$$\begin{aligned}\frac{B_{bi}}{B_{bj}} &= 0.750 \geq 0.75 \quad \mathbf{o.k.} \\ \frac{t_{bi}}{t_{bj}} &= 0.801 \leq 1.0 \quad \mathbf{o.k.} \\ F_y &= F_{yb} \\ &= 46 \text{ ksi} \leq 52 \text{ ksi} \quad \mathbf{o.k.} \\ \frac{F_y}{F_u} &= \frac{F_{yb}}{F_{ub}} \\ &= \frac{46 \text{ ksi}}{58 \text{ ksi}} \\ &= 0.793 \leq 0.8 \quad \mathbf{o.k.}\end{aligned}$$

*Required Strength (Expressed as a Force in a Branch)*

From Chapter 2 of ASCE/SEI 7-05 (ASCE, 2006), the required strength of the connection, expressed as a force in the tension and compression branches (using the LRFD method) is:

$$\begin{aligned} P_u &= 1.2(12.5 \text{ kips}) + 1.6(37.5 \text{ kips}) \\ &= 75.0 \text{ kips} \end{aligned}$$

*Local Yielding of the Branches Due to Uneven Load Distribution*

From AISC *Specification* Section K2.3d, the nominal strength of the overlapping branch for the limit state of local yielding due to uneven load distribution is:

$$P_{n,i} = F_{ybi}t_{bi}(2H_{bi} - 4t_{bi} + b_{eov}) \text{ for } 50\% \leq O_v \leq 80\% \quad (\text{Spec. Eq. K2-18})$$

where:

$$\begin{aligned} b_{eoi} &= \frac{10}{B/t} \left( \frac{F_y t}{F_{ybi} t_{bi}} \right) B_{bi} \leq B_{bi} && (\text{Spec. Eq. K2-20}) \\ &= \frac{10}{17.2} \left[ \frac{46 \text{ ksi } (0.465 \text{ in.})}{46 \text{ ksi } (0.233 \text{ in.})} \right] (3.00 \text{ in.}) \\ &= 3.48 \text{ in.} > B_{bi} = 3.00 \text{ in.} \end{aligned}$$

Therefore, use  $b_{eoi} = 3.00 \text{ in.}$

$$\begin{aligned} b_{eov} &= \frac{10}{B_{bj}/t_{bj}} \left( \frac{F_{ybj} t_{bj}}{F_{ybi} t_{bi}} \right) B_{bi} \leq B_{bi} && (\text{Spec. Eq. K2-21}) \\ &= \frac{10}{13.7} \left[ \frac{46 \text{ ksi } (0.291 \text{ in.})}{46 \text{ ksi } (0.233 \text{ in.})} \right] (3.00 \text{ in.}) \\ &= 2.37 \text{ in.} \leq B_{bi} = 3.00 \text{ in.} \end{aligned}$$

Therefore,  $b_{eov} = 2.37 \text{ in.}$

The nominal strength of the overlapping branch is thus:

$$\begin{aligned} P_{n,i} &= 46 \text{ ksi}(0.233 \text{ in.})[2(5.00 \text{ in.}) - 4(0.233 \text{ in.}) + 3.00 \text{ in.} + 2.73 \text{ in.}] \\ &= 159 \text{ kips} \end{aligned}$$

The nominal strength of the overlapped branch is:

$$\begin{aligned} P_{n,j} &= P_{n,i} \left( \frac{F_{ybj} A_{bj}}{F_{ybi} A_{bi}} \right) && (\text{Spec. Eq. K2-22}) \\ &= 159 \text{ kips} \left[ \frac{5.26 \text{ in.}^2 (46 \text{ ksi})}{3.37 \text{ in.}^2 (46 \text{ ksi})} \right] \\ &= 248 \text{ kips} \end{aligned}$$

The available connection strength, expressed as forces in the tension (overlapping) and compression (overlapped) branches (using the LRFD method), is:

For tension (overlapping) branch:

$$\begin{aligned}\phi P_{n,i} &= 0.95(159 \text{ kips}) \\ &= 151 \text{ kips} \\ 151 \text{ kips} &> 75.0 \text{ kips} \quad \mathbf{o.k.}\end{aligned}$$

For compression (overlapped) branch:

$$\begin{aligned}\phi P_{n,j} &= 0.95(248 \text{ kips}) \\ &= 236 \text{ kips} \\ 236 \text{ kips} &> 75.0 \text{ kips} \quad \mathbf{o.k.}\end{aligned}$$

#### Determine the Required Weld Throat

Assume a continuous weld effective throat will be provided for each branch, and that both branches will be welded around the entire perimeter (including the hidden toe of the overlapped branch).

From AISC *Specification* Section K4.1, the overlapping member effective weld length is:

$$l_{e,i} = 2 \left[ \left( 1 - \frac{O_v}{100} \right) \left( \frac{H_{bi}}{\sin \theta_i} \right) + \frac{O_v}{100} \left( \frac{H_{bi}}{\sin (\theta_i + \theta_j)} \right) + b_{eoi} + b_{eov} \right] \quad (\text{Spec. Eq. K4-11})$$

for  $50\% \leq O_v \leq 80\%$

where  $b_{eoi}$  and  $b_{eov}$  are as shown earlier (*Specification* Equations K2-20 and K2-21) for the limit state of local yielding of the overlapping branch due to uneven load distribution. If  $b_{eoi} = 3.48 \text{ in.} > B_{bi} = 3.00 \text{ in.}$ , then take  $b_{eoi} = 3.00 \text{ in.}$  However, the modified requirements proposed in this report state:

When  $B_{bi}/B > 0.85$  or  $\theta_i > 50^\circ$ ,  $b_{eoi}/2$  shall not exceed  $B_{bi}/4$  and when  $B_{bi}/B_{bj} > 0.85$  or  $(180^\circ - \theta_i - \theta_j) > 50^\circ$ ,  $b_{eov}/2$  shall not exceed  $B_{bi}/4$ .

Thus, use  $b_{eoi} = 2 \left( \frac{B_{bi}}{4} \right) = 1.50 \text{ in.}$

Similarly, when  $\frac{b_{eov}}{2} > B_{bi}/4$ , use  $b_{eov} = 2 \left( \frac{B_{bi}}{4} \right) = 1.50 \text{ in.}$

Therefore, the effective length of the weld to the overlapping branch is:

$$\begin{aligned}l_{e,i} &= 2 \left[ \left( 1 - \frac{6.67}{100} \right) \left( \frac{5.00 \text{ in.}}{\sin 60^\circ} \right) + \frac{6.67}{100} \left( \frac{5.00 \text{ in.}}{\sin (120^\circ)} \right) \right] + 2(1.50 \text{ in.}) \\ &= 2(1.92 \text{ in.} + 3.85 \text{ in.}) + 2(1.50 \text{ in.}) \\ &= 14.54 \text{ in.}\end{aligned}$$

The effective length of the weld to the overlapped branch, when  $B_{bj}/B > 0.85$  or  $\theta_j > 50^\circ$ , is:

$$\begin{aligned}l_{e,i} &= 2(H_{bj} - 1.2t_{bj})/\sin \theta_j \quad (\text{Spec. Table K4.1}) \\ &= 2[6.00 \text{ in.} - 1.2(0.291 \text{ in.})]/\sin 60^\circ \\ &= 13.0 \text{ in.}\end{aligned}$$

Note: A weld should be provided across the widths of the overlapped branch,  $B_{bj}$ , at the toe and the heel (transverse to the chord) even though it is not considered to be at all effective.

The required weld throat, derived from forces in the tension (overlapping) and compression (overlapped) branches, and assuming fillet welds are used, is (using the LRFD method):

For tension (overlapping) branch:

$$\phi P_{nw} = 0.75(F_{nw}t_w l_e)$$

where

$$\begin{aligned} F_{nw} &= 0.60F_{EXX} \\ &= 0.60(70 \text{ ksi}) \\ &= 42 \text{ ksi} \end{aligned}$$

Therefore:

$$\begin{aligned} 0.75(F_{nw}t_w l_e) &\geq 75.0 \text{ kips} \\ t_w &\geq \frac{75 \text{ kips}}{0.75(42 \text{ ksi})(14.54 \text{ in.})} \\ t_w &\geq 0.164 \text{ in.} \end{aligned}$$

For the compression (overlapped) branch:

$$\begin{aligned} t_w &\geq \frac{75 \text{ kips}}{0.75(42 \text{ ksi})(13.0 \text{ in.})} \\ t_w &\geq 0.183 \text{ in.} \end{aligned}$$

### Discussion:

If fillet welds were designed to develop the branch member yield strength at all locations around the branch perimeter in accordance with AISC 360-10 (2010), the required weld throat would be as follows:

For the tension (overlapping) branch:

$$\begin{aligned} \phi P_{nw} &\geq \phi P_{n,i} \\ 0.75(F_{nw})(A_{we}) &\geq 0.90(F_{ybi})(t_{bi}) \\ 0.75(42 \text{ ksi})(t_w) &\geq 0.90(46 \text{ ksi})(t_{bi}) \\ t_w &\geq 1.31(t_b) = 0.305 \text{ in.} \end{aligned}$$

For the compression (overlapped) branch:

$$t_w \geq 1.31(t_b) = 0.381 \text{ in.}$$

In the preceding calculations, the branch design wall thickness has been used. The overlapping (tension) branch is loaded to 50% of its factored yield load, and thus the excessively large weld sizes required to develop the branch yield strength are not necessary. As shown previously, the required weld throat calculated using the recommendations of this paper is approximately 50% smaller than the required weld throat to develop the branch yield strength. This is true also for the overlapped (compression) branch, which carries only a fraction of its yield load.

## ACKNOWLEDGMENTS

Financial support for this project was provided by the American Institute of Steel Construction, the Natural Sciences and Engineering Research Council of Canada (NSERC), and the Canadian Institute of Steel Construction Education and Research Council. Fabrication was provided, as a gift in-kind, by Walters Inc., Hamilton, Ontario, and the hollow structural sections used were donated by Atlas Tube, Harrow, Ontario.

## SYMBOLS AND ABBREVIATIONS

$A$	Cross-sectional area of the rectangular HSS chord member, in. <sup>2</sup>	$M_L$	Bending moment due to live load, kip-in.
$A_b$	Cross-sectional area of the rectangular HSS branch member, in. <sup>2</sup>	$NDT$	Nondestructive test
$B$	Overall width of rectangular HSS chord member, measured normal to the plane of the connection, in.	$O_v$	Overlap (%) = $(q/p \times 100)$ %
$B_b$	Overall width of rectangular HSS branch member, measured normal to the plane of the connection, in.	$P_D$	Axial force due to dead load, kips
$B_{bi}$	Overall width of the overlapping branch, in.	$P_L$	Axial force due to live load, kips
$B_{bj}$	Overall width of the overlapped branch, in.	$P_a$	Actual weld fracture load, kips
$COV$	Coefficient of variation	$P_n$	Predicted weld fracture load, kips
$E$	Young's modulus of the rectangular HSS, ksi	$P_{n,i}$	Nominal axial strength of the overlapping branch, kips
$F_{EXX}$	Electrode classification number, ksi	$P_{n,j}$	Nominal axial strength of the overlapped branch, kips
$F_{nw}$	Nominal strength of the weld metal per unit area, ksi	$P_{nw}$	Nominal resistance of the weld, kips
$F_y$	Specified minimum yield stress of rectangular HSS chord, ksi	$P_u$	Required axial strength in tension or compression, kips
$F_{yb}$	Specified minimum yield stress of rectangular HSS branch, ksi	$SG$	Strain gage
$F_{ybi}$	Specified minimum yield stress of the overlapping branch, ksi	$b_{eoi}$	Effective width of the branch face welded to the chord, in.; effective length of the weld to the chord, in.
$F_{ybj}$	Specified minimum yield stress of the overlapped branch, ksi	$b_{eov}$	Effective width of the branch face welded to the overlapped branch, in.; effective length of the weld to the chord, in.
$H$	Overall height of rectangular HSS chord member, measured in the plane of the connection, in.	$d$	Greatest perpendicular dimension measured from a line flush to the base metal surface to the weld surface, in.
$H_b$	Overall height of rectangular HSS branch member, measured in the plane of the connection, in.	$e$	Eccentricity in a truss connection, positive being away from the branches, in.
$H_{bi}$	Overall depth of the overlapping branch, in.	$i$	Subscript/ term used to identify the overlapping branch member; Subscript/ term used to identify weld elements
$H_{bj}$	Overall depth of the overlapped branch, in.	$j$	Subscript/term used to identify the overlapped branch member
$LVDT$	Linearly varying differential transformer	$l_e$	Effective length of groove and fillet welds for rectangular HSS, in.
$M_D$	Bending moment due to dead load, kip-in.	$m_R$	Mean of the ratio (actual element strength/nominal element strength)
		$p$	Projected length of the overlapping branch on the connecting face of the chord, in.
		$q$	Overlap length, measured along the connecting face of the chord beneath the region of overlap of the branches, in.
		$t$	Wall thickness of rectangular HSS chord member, in.

$t_b$	Wall thickness of rectangular HSS branch member, in.
$t_{bi}$	Wall thickness of the overlapping branch member, in.
$t_{bj}$	Wall thickness of the overlapped branch member, in.
$t_w$	Weld effective throat, in.
$\alpha$	Coefficient of separation (taken to be 0.55)
$\beta$	Width ratio; the ratio of overall branch width to chord width for rectangular HSS
$\beta^+$	Safety index
$\epsilon_{avg}$	Average strain, in./in.
$\epsilon_{rup}$	Strain at rupture, in./in.
$\phi$	Resistance factor (associated with the load and resistance factor design method)
$\theta_i$	Included angle between the overlapping branch and chord, degrees
$\theta_j$	Included angle between the overlapped branch and chord, degrees

## REFERENCES

- AISC (2010), *Specification for Structural Steel Buildings*, ANSI/AISC 360-10, American Institute of Steel Construction, Chicago, IL.
- AISC (2011), *Steel Construction Manual*, 14th ed., American Institute of Steel Construction, Chicago, IL.
- ASCE (2006), *Minimum Design Loads for Buildings and Other Structures*, ASCE/SEI 7-05, American Society of Civil Engineers, Reston, VA.
- ASTM (2009), *Standard Test Methods and Definitions for Mechanical Testing of Steel Products*, ASTM A370-09, American Society for Testing Materials, West Conshohocken, PA.
- ASTM (2013), *Standard Specification for Cold-Formed Welded Carbon Steel Hollow Structural Sections (HSS)*, ASTM A1085-13, West Conshohocken, PA. American Society for Testing Materials.
- AWS (2010), *Structural Welding Code—Steel*, 22, ANSI/AWS D1.1/D1.1M:2010, American Welding Society, Miami, FL.
- CSA (2013), *General Requirements for Rolled or Welded Structural Quality Steel*, G40.20-13/G40.21-13, Canadian Standards Association, Toronto, Canada.
- Davies, G. and Packer, J.A. (1982), “Predicting the Strength of Branch Plate—RHS Connections for Punching Shear,” *Canadian Journal of Civil Engineering*, Vol. 9, No. 3, pp. 458–467.
- Fisher, J.W., Galambos, T.V., Kulak, G.L. and Ravindra, M.K. (1978), “Load and Resistance Factor Design Criteria for Connectors,” *Journal of the Structural Division*, ASCE, Vol. 104, No. 9, pp. 1427–1441.
- Frater, G.S. (1991), “Performance of Welded Rectangular Hollow Structural Section Trusses,” Ph.D. Thesis, University of Toronto, Toronto, Canada.
- Frater, G.S. and Packer, J.A. (1992a), “Weldment Design for RHS Truss Connections, I: Applications,” *Journal of Structural Engineering*, ASCE, Vol. 118, No. 10, pp. 2784–2803.
- Frater, G.S. and Packer, J.A. (1992b), “Weldment Design for RHS Truss Connections, II: Experimentation,” *Journal of Structural Engineering*, ASCE, Vol. 118, No. 10, pp. 2804–2820.
- Frater, G.S. and Packer, J.A. (1992c), “Modelling of Hollow Structural Section Trusses,” *Canadian Journal of Civil Engineering*, Vol. 19, No. 6, pp. 947–959.
- IIW (1989), *Design Recommendations for Hollow Section Joints—Predominantly Statically Loaded*, 2nd ed., Doc. XV-701-89. International Institute of Welding, Paris, France.
- IIW (2012), *Static Design Procedure for Welded Hollow Section Joints—Predominantly Statically Loaded*, 3rd ed., Doc. XV-1402-12, International Institute of Welding, Paris, France.
- ISO (2013), *Static Design Procedure for Welded Hollow-Section Joints—Recommendations*, ISO 14346:2013(E), International Standards Organization, Geneva, Switzerland.
- McFadden, M.R. and Packer, J.A. (2014), “Effective Weld Properties for Hollow Structural Section T-Connections under Branch In-Plane Bending,” *Engineering Journal*, AISC, Vol. 51, No. 4, pp. 247–266.
- McFadden, M.R., Sun, M. and Packer, J.A. (2013), “Weld Design and Fabrication for RHS Connections,” *Steel Construction*, Vol. 6, No. 1, pp. 5–10.
- Mehrotra, B.L. and Govil, A.K. (1972), “Shear Lag Analysis of Rectangular Full-Width Tube Connections,” *Journal of the Structural Division*, ASCE, Vol. 98, No. ST1, pp. 287–305.
- Packer, J.A. and Cassidy, C.E. (1995), “Effective Weld Length for HSS T, Y, and X Connections,” *Journal of Structural Engineering*, ASCE, Vol. 121, No. 10, pp. 1402–1408.

Packer, J.A. and Frater, G.S. (2005), "Recommended Effective Throat Sizes for Flare Groove Welds to HSS," *Engineering Journal*, AISC, Vol. 42, No. 1, pp. 31–44.

Packer, J.A., Wardenier, J., Zhao, X.L., van der Vegte, G.J. and Kurobane, Y. (2009), *Design Guide for Rectangular Hollow Section (RHS) Joints under Predominantly Static Loading*, 2nd ed., CIDECT DG 3, CIDECT, Geneva, Switzerland.

Ravindra, M.K. and Galambos, T.V. (1978), "Load and Resistance Factor Design for Steel," *Journal of the Structural Division*, ASCE, Vol. 104, No. 9, pp. 1337–1353.

